Cancer Science
Japanese Cancer Association JCA
Open Access

Requisite role of vasohibin-2 in spontaneous gastric cancer formation and accumulation of cancer-associated fibroblasts

Yasuhiro Suzuki,[1] Shuji Kitahara,[2,3] Takuya Suematsu,[1] Masanobu Oshima[4] and Yasufumi Sato[1]

[1]Department of Vascular Biology, Institute of Development, Aging and Cancer, Tohoku University, Sendai, Miyagi, Japan; [2]Department of Radiation Oncology, Massachusetts General Hospital, Harvard Medical School, Boston, Massachusetts, USA; [3]Department of Anatomy and Developmental Biology, School of Medicine, Tokyo Women's Medical University, Tokyo; [4]Division of Genetics, Cancer Research Institute, Kanazawa University, Kanazawa, Ishikawa, Japan

Key words

Cancer-associated fibroblasts, epiregulin, gastric cancer, interleukin-11, vasohibin-2

Correspondence

Yasuhiro Suzuki, Department of Vascular Biology, Institute of Development, Aging, and Cancer, Tohoku University, 4-1 Seiryo-machi, Aoba-ku, Sendai 980-9575, Japan.
Tel: +81-22-717-8532; Fax: +81-22-717-8533;
E-mail: yasuhiro.suzuki.d4@tohoku.ac.jp

Funding Information

Japan Society for the Promotion of Science (Grant / Award Number: 15K06821, 24501309).

Received May 1, 2017; Revised August 30, 2017; Accepted September 18, 2017

Cancer Sci **108** (2017) 2342–2351

doi: 10.1111/cas.13411

The vasohibin (VASH) family consists of two genes, *VASH1* and *VASH2*. VASH1 is mainly expressed in vascular endothelial cells and suppresses angiogenesis in an autocrine manner, whereas VASH2 is mainly expressed in cancer cells and exhibits pro-angiogenic activity. Employing adenomatous polyposis coli gene mutant mice, we recently reported on the role of Vash2 in the spontaneous formation of intestinal tumors. In this study, we used K19-Wnt1/C2mE (*Gan*) mice and examined the role of Vash2 in spontaneous gastric cancer formation. *Gan* mice spontaneously develop gastric tumors by activation of Wnt and prostaglandin E2 signaling pathways in gastric mucosa after 30 weeks of age. Expression of *Vash2* mRNA was significantly increased in gastric tumor tissues compared with normal stomach tissues. When *Gan* mice were crossed with the *Vash2*-deficient (*Vash2*$^{LacZ/LacZ}$) strain, gastric cancer formation was significantly suppressed in *Vash2*$^{LacZ/LacZ}$ *Gan* mice. Normal composition of gastric mucosa was partially maintained in *Vash2*$^{LacZ/LacZ}$ *Gan* mice. Knockout of *Vash2* caused minimal reduction of tumor angiogenesis but a significant decrease in cancer-associated fibroblasts (CAF) in tumor stroma. DNA microarray analysis and real-time RT-PCR showed that mRNA levels of epiregulin (Ereg) and interleukin-11 (Il11) were significantly downregulated in gastric tumors of *Vash2*$^{LacZ/LacZ}$ *Gan* mice. Furthermore, conditioned medium of gastric cancer cells stimulated migration of and α-smooth muscle actin expression in fibroblasts, whereas conditioned medium of VASH2 knockdown cells attenuated these effects *in vitro*. These results suggest that VASH2 plays an important role in gastric tumor progression via the accumulation of CAF accompanying upregulation of EREG and IL-11 expression.

Gastric cancer is the third leading cause of cancer-related death in Japan. Risk factors for gastric cancer include *Helicobacter pylori* infection, host genetic susceptibility and other environmental factors, and multiple genetic mutations, epigenetic alterations and aberrant molecular signaling pathways are involved in its development.[1]

The treatment of gastric cancer has evolved in the past three years. Molecular characterization of gastric cancer has provided clues for treatment development, and the introduction of agents targeting human epidermal growth factor (EGF) receptor 2 and vascular endothelial growth factor (VEGF) family/VEGF receptor has brought this disease into the era of molecular and personalized medicine.[2]

We searched for and isolated novel angiogenesis regulators that we have designated as vasohibin-1 (VASH1) and vasohibin-2 (VASH2). VASH1 is an endothelium-derived angiogenesis inhibitor,[3] whereas VASH2 is a homologue of VASH1 that acts as an angiogenesis stimulator.[4,5] These two regulators are devoid of the classical secretory signal sequence but are efficiently secreted when they form a complex with small vasohibin-binding protein.[6,7] Of note, VASH2 is produced by cancer cells such as ovarian carcinoma, hepatocellular carcinoma and intestinal adenocarcinoma, and promotes tumor growth by stimulating tumor angiogenesis.[8–10] Using xenograft models of human ovarian cancer, we recently reported that targeting of VASH2 by exogenous administration of siRNA or a neutralizing antibody specific for VASH2 inhibits tumor growth by attenuating tumor angiogenesis.[11,12] Furthermore, when an experimental model for spontaneous adenomatous polyposis, the adenomatous polyposis coli multiple intestinal neoplasia (*Apc*$^{Min/+}$) mouse, is crossed with the *Vash2*$^{lacZ/lacZ}$ mouse, the number of intestinal tumors significantly decreases in association with normalization of tumor vessels.[10] The expression of VASH2 has also been documented in human gastric cancer cell lines,[13] but the significance of VASH2 in gastric cancer development is not well defined.

Spontaneous carcinogenic mouse models are useful for gaining insight into the pathogenesis and molecular mechanisms of cancers. The *K19-Wnt1/C2mE* (*Gan* for Gastric neoplasia) mouse was recently established by the transgenic expression of

Wnt1, cyclooxygenase-2 and microsomal prostaglandin E synthase-1 under a *Keratin 19* promoter in gastric epithelial cells, recapitulating human gastric tumors not only in terms of molecular mechanism but also tumor pathology.[14] Here we used *Gan* mice, crossed with *Vash2*$^{lacZ/lacZ}$ mice, and examined the significance of VASH2 in gastric tumor growth and the tumor stromal microenvironment.

Materials and Methods

Mouse models. As noted, *Gan* mice highly express Wnt1, cyclooxygenase-2 and microsomal prostaglandin E synthase-1 under *Keratin 19* promoter activity in gastric epithelial cells and generate gastric tumors after 30 weeks of birth, as previously reported.[14] *Vash2*$^{LacZ/LacZ}$ mice were maintained as described earlier,[4] and *Gan* mice were mated with *Vash2*$^{LacZ/LacZ}$ mice to generate *Vash2*$^{LacZ/LacZ}$ *Gan* mice. For the tumor development analyses, mice were euthanized and examined at 30 weeks of age. All animal experiments were carried out according to the protocol approved by the Committee on Animal Experimentation of Tohoku University, Japan.

Histological and immunohistochemical analyses. *Gan* mice at age 30 weeks were anesthetized and transcardially perfused with PBS followed by 4% paraformaldehyde. Stomachs were extracted and incubated overnight with 4% paraformaldehyde, dehydrated in graded ethanol and xylene, and embedded in paraffin wax. Vertical sections (5 μm) of the entire gastric mucosa were prepared for conventional H&E staining or immunohistochemical staining. For immunohistochemical staining, tissue sections were autoclaved in citrate buffer (pH 6.0) for 5 min for antigen retrieval prior to incubation with primary antibodies. Antibodies against the H^+, K^+-ATPase (MBL, Nagoya, Japan), F4/80 (Serotec, Oxford, UK), alpha smooth muscle actin (αSMA; Sigma, St. Louis, MO, USA), Tenascin-C (TNC; Abcam, Cambridge, MA, USA), Ki-67, CD31 and Vimentin (VIM; Cell Signaling, Beverly, MA, USA) were used as the primary antibodies. Staining signals were visualized using Histofine Simple Stain MAX PO (Nichirei, Tokyo, Japan) followed by counterstaining with hematoxylin. Microphotographs were obtained using an MC120 HD camera attached to a Leica DM 2000 LED microscope (Leica Microsystems K.K., Tokyo, Japan). For fluorescence immunostaining, antibodies conjugated with Alexa Fluor 488 or Alexa Fluor 555 (Thermo Fisher Scientific, Waltham, MA, USA) were used as the secondary antibodies. Nuclei were then counterstained using ToPro-3 (Thermo Fisher Scientific). Fluorescence images were captured using a Fluoview FV1000 confocal microscope system (Olympus, Tokyo, Japan).

Measurement of mucosal thickness. The mucosal thickness of gastric tumors was measured from micrographs of H&E-stained vertical sections of entire gastric tumors using LAS Software (Leica Microsystems K.K.). Relative mucosal thickness of samples from *Vash2*$^{LacZ/LacZ}$ *Gan* mice was calculated in comparison with the mean of the control *Gan* mice.

***In situ* hybridization.** *In situ* hybridization was performed with the ISH Reagent Kit (Genostaff, Tokyo, Japan) according to the manufacturer's instructions. Tissue sections were de-paraffinized with G-Nox and rehydrated through an ethanol series and PBS. The sections were: fixed with 10% NBF (10% formalin in PBS) for 15 min at room temperature (RT) and washed in PBS; treated with 4 μg/mL Proteinase K (Wako Pure Chemical, Osaka, Japan) in PBS for 10 min at 37°C and washed in PBS; re-fixed with 10% NBF for 15 min at RT and washed in PBS; placed in 0.2 N HCl for 10 min at RT and washed in PBS; and placed within a Coplin jar containing 1× G-Wash (Genostaff), equal to 1× SSC. Hybridization was performed with probes corresponding to the nucleotide positions 1321–2001 of mouse *Vash2* mRNA (GenBank accession number NM_144879.2) at concentrations of 300 ng/mL in G-Hybo-L (Genostaff) for 16 h at 60°C. After hybridization, the sections were washed in 1× G-Wash for 10 min at 60°C and 50% formamide in 1× G-Wash for 10 min at 60°C.

Sections then were washed twice in 1× G-Wash for 10 min at 60°C, twice in 0.1× G-Wash for 10 min at 60°C, and twice in TBST (0.1% Tween20 in TBS) at RT. After treatment with 1× G-Block (Genostaff) for 15 min at RT, the sections were incubated with anti-digoxigenin AP conjugate (Roche Diagnostics, Mannheim, Germany) diluted 1:2000 with ×50G-Block (Genostaff) in TBST for 1 h at RT. The sections were washed twice in TBST and then incubated in 100 mM NaCl, 50 mM $MgCl_2$, 0.1% Tween20, 100 mM Tris-HCl, pH 9.5. Coloring reactions were performed with NBT/BCIP solution (Sigma-Aldrich, St. Louis, MO, USA) overnight and then washed in PBS. The sections were counterstained with Kernechtrot stain solution (Muto Pure Chemicals, Tokyo, Japan) and mounted with G-Mount.

RT-PCR and quantitative real-time RT-PCR. Total RNA was extracted from mouse tissues and cultured cells using QIAzol Lysis Reagent (QIAGEN, Hilden, Germany) and purified using the RNeasy Mini Kit (QIAGEN). First-strand cDNA was synthesized by reverse transcriptase using ReverTra Ace (TOYOBO, Osaka, Japan). PCR was performed using sets of primers specific for the target genes described below. Thermal cycler conditions were 20–30 cycles at 94°C for 15 s for denaturing, at 56°C for 30 s for annealing, and at 72°C for 45 s for extension. PCR products were separated on a 1% agarose gel and visualized under ultraviolet by ethidium bromide staining. Quantitative real-time RT-PCR was performed using the CFX96 real-time RT-PCR detection system (Bio-Rad Laboratories, Hercules, CA, USA) according to the manufacturer's instructions. PCR conditions consisted of an initial denaturation step at 95°C for 3 min, followed by 40 cycles of 10 s at 95°C, 10 s at 56°C and 30 s at 72°C. Relative mRNA levels of target genes were normalized to beta-2-microglobulin (*B2m*) mRNA level. The specific primer pairs for target genes are summarized in Table S1. Specific primer pairs for detection of *CD44* splicing variant (*CD44v*) targeted exons 5 and 16 of *CD44* mRNA.[15]

Microarray analysis. Total RNA was extracted from gastric tumor tissues as described above. The quality of total RNA was confirmed by an Agilent 2100 Bioanalyzer (Agilent Technologies, Santa Clara, CA, USA). The cRNA was synthesized and labeled with Cy3 using the Low Input Quick-Amp Labeling Kit (Agilent Technologies). The Cy3-labeled cRNA samples were subjected to hybridization to SurePrint G3 Mouse GE Microarray chips (Agilent Technologies) using a Gene Expression Hybridization Kit. Fluorescence signals in the chips were detected by an Agilent microarray scanner (Agilent Technologies) and quantified using Feature Extraction software (Agilent Technologies).

Cell cultures. FU97 cells (a human stomach cancer cell line) and SF-TY cells (a human skin fibroblast cell) were obtained from the Japanese Collection of Research Bioresources Cell Bank (Osaka, Japan). FU97 cells were cultured in DMEM (Wako Pure Chemical) supplemented with 10% heat-inactivated FBS (SAFC Biosciences, Lenexa, KS, USA) and 10 μg/mL of recombinant human insulin (Wako Pure Chemical). SF-TY cells were maintained in DMEM supplemented with 10% FBS and non-essential amino acids.

Knockdown of VASH2 by shRNA. FU97 cells were transfected with the VASH2 shRNA expression vector or its control mock vector using FuGENE HD Transfection Reagent (Promega, Madison, WI, USA) and were selected in culture medium containing 10 μg/mL puromycin (Wako Pure Chemical), as reported previously.[8]

Fibroblast proliferation and migration. FU97 cells and VASH2 knockdown (shVASH2) clones were plated in 60-mm dishes at 5×10^5 cells and cultured overnight in the culture medium. The following day, the medium was replaced by DMEM containing 0.5% FBS. The conditioned medium was collected 48 h later and filtered through a MILLEX-GP PES 0.22-μm filter (Millipore, Bedford, MA, USA). Cell proliferation was measured using a BrdU Cell Proliferation ELISA Kit (Abcam). Cells were plated in a 96-well plate at 5×10^3 cells per well and starved in DMEM containing 0.5% FBS for 16 h. Cells were then treated with conditioned media (CM) from FU97 cells or shVASH2 clones and labeled with BrdU for 24 h. Incorporated BrdU was detected according to the manufacturer's instructions. Migratory activity of fibroblasts was measured by modified Boyden chamber assay.[6] SF-TY cells were seeded on the upper chambers (inserts) of the Boyden chamber (8.0 μm pore size, Corning) at 2×10^5 cells. The lower chamber was filled with 600 μL of CM from FU97 cells or shVASH2 clones. After incubation for 4 h, SF-TY cells that migrated across the membrane were fixed with methanol, stained with DAPI (Sigma-Aldrich), and counted in nine fields per insert in a blinded manner.

Statistical analysis. Data are expressed as mean ± SD and were analyzed using unpaired Student's *t*-tests. A value of $P < 0.05$ was considered to denote statistical significance.

Results

Increased expression of VASH2 in gastric tumor cells in *Gan* mice. Previous reports demonstrated that VASH2 is highly expressed in various types of human tumor tissues as well as in established cancer cell lines.[8,9,13,16–20] Shen *et al.*[13] reported that both human gastric cancer cell lines and experimentally prepared tumor-associated macrophages express *VASH2* mRNA in an *in vitro* culture system. However, the roles of VASH2 in spontaneous gastric tumor growth are not fully understood. *Gan* mice spontaneously generate gastric tumors by simultaneous signal activation of both Wnt and prostaglandin E2 (PGE_2) in gastric epithelia under keratin-14 promoter activity.[21–27] We first examined the expression level of *Vash2* mRNA in gastric tumors spontaneously developed in *Gan* mice at 30 weeks of age. As shown in Figure 1(a), RT-PCR analysis showed enhanced expression of *CD44* splicing variants (*CD44v*) and *Vash2* in gastric tumors of *Gan* mice, whereas normal stomach tissues expressed low levels of *Vash2* and no *CD44v*, as previously reported.[15,28] According to *CD44v* mRNA expression, increased expression of *Vash2* mRNA was detected in *Gan* mice gastric tumors (Fig. 1a). Real-time RT-PCR analysis showed that the expression level of *Vash2* mRNA in *Gan* mouse gastric tumors was approximately three times higher than in normal stomachs of wild-type mice (Fig. 1b).

We then performed *in situ* hybridization for mouse *Vash2* transcript in tissue sections of *Gan* mouse gastric tumors at 30 weeks of age. Signals for *Vash2* mRNA transcripts visualized by antisense probes were detected in gastric tumors of *Gan* mice but not in normal stomach (Fig. 1c). As shown in Figure 1(d), the signals were mainly localized in dysplastic epithelial cells (black arrowheads), whereas they were hardly observed in other stromal cells (white arrowheads). These results indicate that dysplastic epithelial cells express *Vash2* mRNA in *Gan* mice.

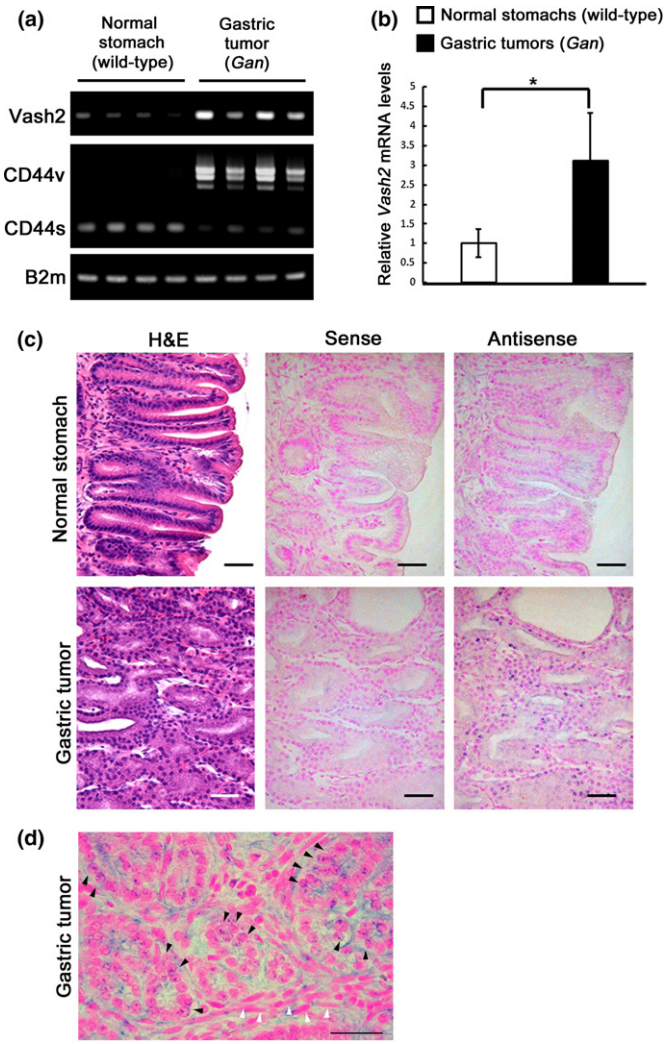

Fig. 1. Expression of *Vash2* mRNA in gastric tumors. (a) RT-PCR for *CD44* and *Vash2* mRNA in the normal stomachs of wild-type mice ($n = 4$) and gastric tumors of *Gan* mice ($n = 4$) at 30 weeks of age. The expression level of *B2m* mRNA was used as an internal control. PCR products of CD44 show three types of splicing variant isoforms (CD44v) and standard form (CD44s).[15,28] (b) The relative expression level of *Vash2* mRNA in *Gan* mouse gastric tumors ($n = 4$) at 30 weeks of age compared to wild-type normal stomachs ($n = 4$). The expression level of *Vash2* mRNA was normalized to the *B2m* mRNA level. Mean ± SD shown. *$P < 0.05$ versus wild-type. (c) *In situ* hybridization of *Vash2* mRNA in *Gan* mouse gastric tumor tissue. Mouse *Vash2*-specific antisense and sense probes were hybridized with cross-sections of *Gan* mouse gastric tumors and normal stomach at 30 weeks of age. Representative images with antisense (right) and sense (center) are shown. The left panel shows representative images of H&E staining. Scale bar: 100 μm. (d) A high magnification micrograph showing *Vash2*-expressing dysplastic epithelial cells (black arrowheads) in Gan mouse gastric tumors. White arrowheads indicate stromal cells. Scale bar: 100 μm.

Suppression of gastric tumor growth in *Vash2*-deficient *Gan* mice. To investigate the role of VASH2 in spontaneous gastric tumor development, we bred *Gan* mice with *Vash2*-deficient mice ($Vash2^{LacZ/LacZ}$) to obtain *Vash2*-deficient *Gan* mice ($Vash2^{LacZ/LacZ}$ *Gan*) and examined the phenotypic differences

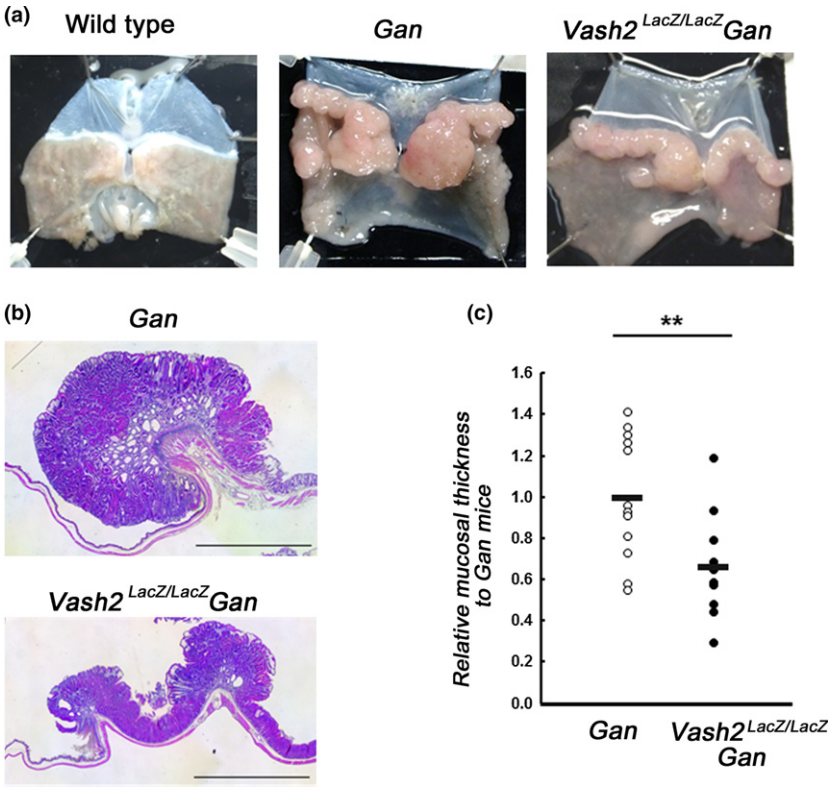

Fig. 2. Suppression of gastric tumor growth by knockout of the *Vash2* gene. (a) Representative macroscopic images of wild-type normal stomach and *Gan* and *Vash2*$^{LacZ/LacZ}$ *Gan* mouse gastric tumors at 30 weeks of age. (b) Representative images of H&E staining of *Gan* mouse (top) and *Vash2*$^{LacZ/LacZ}$ *Gan* mouse (bottom) gastric tumors at 30 weeks of age. Scale bar: 2 mm. (c) Relative gastric mucosal thickness of *Vash2*$^{LacZ/LacZ}$ *Gan* mouse gastric tumors (n = 11) to the mean level of *Gan* mouse tumors (n = 12) at 30 weeks of age. Each circle indicates the relative tumor thickness of individual mice. $^{**}P < 0.01$ versus *Gan* mouse tumors.

in gastric tumors developed in those mice. As shown in Figure 2(a), development of gastric tumors was observed in *Gan* mice at 30 weeks of age, as reported previously.[14] Of note, gastric tumor growth was obviously suppressed in *Vash2*$^{LacZ/LacZ}$ *Gan* mice compared with that in *Gan* mice (Fig. 2a,b). The mean of histologic tumor thickness was significantly reduced by knockout of *Vash2* (Fig. 2b,c).

Immunohistochemical staining for Ki-67 antigen in paraffin sections of those gastric tumor tissues showed that Ki-67-positive proliferating cells were frequently observed in the entire gastric dysplastic epithelia of *Gan* mice tumors, whereas most proliferating cells were limited to the proliferating zone at the gland neck area in gastric tumors of *Vash2*$^{LacZ/LacZ}$ *Gan* mice (Fig. 3a,c). To confirm the distribution of gastric parietal cells in gastric tumors, we performed immunostaining with antibody for the proton pump (H^+, K^+-ATPase), used as a marker of parietal cells. As shown in the center panel of Figure 3(b), a small number of gastric parietal cells was observed in *Gan* mice gastric tumors (Fig. 3d), indicating an architectural disorder of gastric tumor tissues, as reported previously.[25] However, a numerous parietal cell population was still maintained in gastric tumors of *Vash2*$^{LacZ/LacZ}$ *Gan* mice (Fig. 3b,d). These results indicate that the lack of the *Vash2* gene suppressed spontaneous gastric cancer development.

Effect of Vash2 on stromal activation in gastric cancer. The tumor stromal microenvironment (e.g. tumor angiogenesis, expansion of cancer associated fibroblasts (CAF) and infiltration of immune cells) plays crucial roles in tumor development and progression. Therefore, we examined whether *Vash2* deficiency might affect the stromal microenvironment in gastric tumors. Immunofluorescence staining of tissue sections of *Gan* mouse gastric tumors with anti-CD31 antibody showed that a large number of capillary blood vessels are generated in these tumors (Fig. 4a, left panel). In comparison with *Gan* mice, slightly fewer capillaries were observed in gastric tumors of *Vash2*$^{LacZ/LacZ}$ *Gan* mice (Fig. 4a, right panel), but overall this difference was not statistically significant (Fig. 4b). Tumor blood vessels are typically fragile and leaky because of their immature structure accompanied by poor pericyte coverage. We previously reported that *Vash2* depletion causes vascular normalization with restoration of pericyte coverage.[10,17] However, *Vash2* deficiency did not affect pericyte coverage in the *Gan* mouse model (data not shown). Inflammatory responses via infiltrated monocytes/macrophages also have a critical effect on spontaneous gastric tumor growth. Immunohistochemical staining for the F4/80 antigen, a marker specific for mouse macrophages, revealed numerous macrophages infiltrating into gastric tumor stroma in *Vash2*$^{LacZ/LacZ}$ *Gan* and *Gan* mouse tumors (Fig. 4c,d), suggesting that *Vash2* disruption might not affect macrophage infiltration in this mouse model.

Next, we evaluated the expansion of CAF in gastric tumor stroma by immunostaining for αSMA and VIM. Numerous VIM-positive and/or αSMA-positive CAF were detected in entire *Gan* mouse tumor tissues, whereas CAF were sparsely observed in *Vash2*$^{LacZ/LacZ}$ *Gan* tumors (Fig. 5a,b). Immunofluorescence staining for another CAF marker, Tenascin C (TNC), also showed that *Vash2* deficiency significantly reduced the stromal expansion of TNC-positive CAF (Fig. 5c, d) compared with *Gan* mice. These results suggested that VASH2 produced by tumor cells might accelerate the expansion of CAF into tumor stroma in addition to its pro-angiogenic activity.

Downregulation of expression of Epiregulin and interleukin-11 by *Vash2* depletion in gastrointestinal tumors. To identify genes with expression changes in gastric tumor tissues by knockout of the *Vash2* gene, we comprehensively compared mRNA expression profiles between *Gan* mouse gastric tumors and *Vash2*$^{LacZ/LacZ}$ *Gan* mouse gastric tumors by a DNA

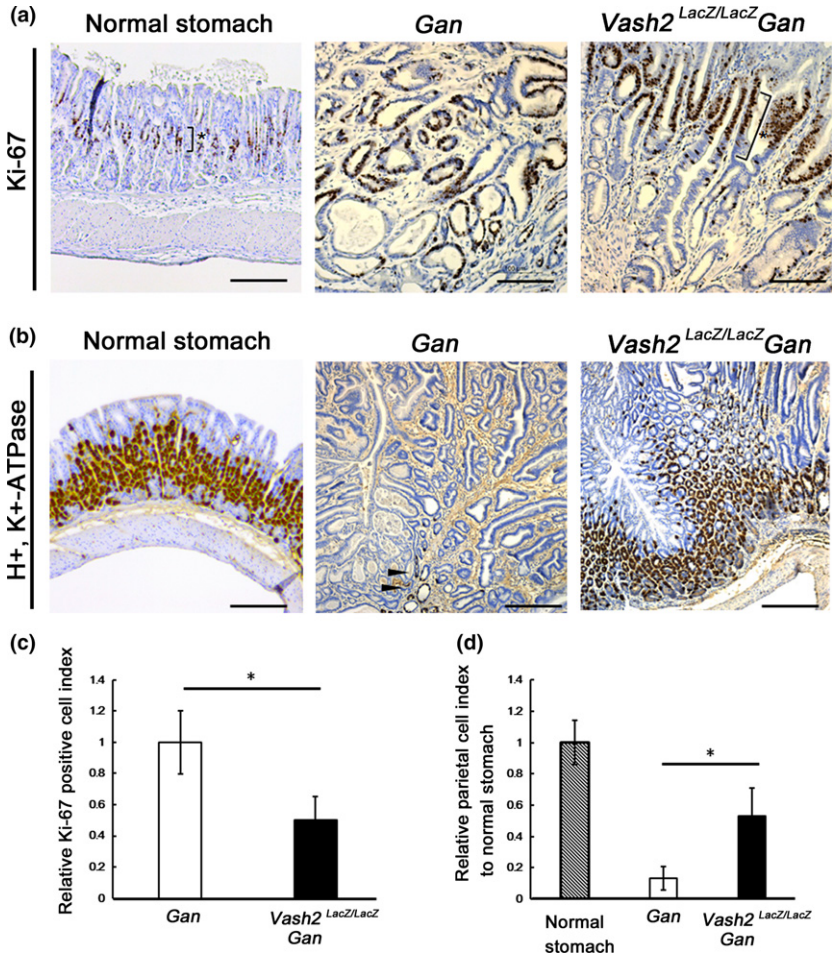

Fig. 3. Effect of *Vash2* depletion on proliferation of gastric tumor cells and population of gastric parietal cells. (a, b) Representative images of immunohistochemical staining for Ki-67 antigen (a) and H+, K+-ATPase (b) of normal stomach (left), *Gan* mouse (center) and *Vash2*$^{LacZ/LacZ}$ *Gan* mouse (right) gastric tumors. Asterisk in (a) shows the proliferating zone in the gland neck area. Arrowheads in (b) indicate H+, K+-ATPase expressing gastric parietal cells. Scale bars: 200 μm. (c) Relative Ki-67 positive dysplastic epithelial cell index in *Vash2*$^{LacZ/LacZ}$ *Gan* mice to that in *Gan* mouse ($n = 6$ fields analyzed from three independent animals). (d) Relative parietal cell index in *Gan* mouse and *Vash2*$^{LacZ/LacZ}$ *Gan* mouse gastric tumors to that in normal stomachs ($n = 6$ fields analyzed from three independent animals). All quantitative data show mean ± SD. *$P < 0.05$ versus Gan mouse tumors.

microarray analysis. In *Vash2*$^{LacZ/LacZ}$ *Gan* mouse gastric tumors, 11 genes were upregulated (>2.0 fold) and 164 genes downregulated (<0.5 fold) compared with *Gan* mouse gastric tumors (Tables S2 and S3). Functional classification by Gene Ontology terms showed that upregulated genes were enriched for circadian rhythmic processes corresponding to *Dbp*, *Hlf*, *Per3* and *Tef*. Indeed, real-time RT-PCR analysis showed that mRNA expression levels of *Hlf* and *Dbp* were significantly upregulated in *Vash2*$^{LacZ/LacZ}$ *Gan* mouse tumors compared to *Gan* mouse tumors (Fig. 6a). In contrast hand, Gene Ontology terms for downregulated genes were classified to many functions, including regulation of gene expression, biosynthesis, cell proliferation and defense response. Downregulation of stem cell/cancer stem cell markers (*CD44* and *CD133*) and vascular endothelial cell markers (*Edn1* and *Tie2*) correlated with the suppression of cancer cell proliferation and tumor angiogenesis caused by *Vash2* disruption, as shown in Figures 3(a) and 4(a), respectively. A significant reduction in mRNA levels of *CD44* and *CD133* was confirmed by real-time RT-PCR analysis (Fig. 6b), whereas *Vash2* deficiency did not significantly change mRNA levels of vascular endothelial cell markers and typical angiogenic factors, such as *Vegfa* and fibroblast growth factor 2 (*Fgf2*) (Fig. 6c,d). Here, we focused on interleukin-11 (*IL-11*, a member of the IL-6 family) and Epiregulin (*Ereg*, a member of the EGF family), listed in Table S3 as downregulated genes, because previous reports suggested that CAF might promote gastrointestinal tumor growth through production of IL-6 family and EGF family.[21,22,29–32] By real-time RT-PCR analysis we confirmed that the mRNA expression levels of *Ereg*, *Il11* and *Il6* were significantly reduced in *Vash2*$^{LacZ/LacZ}$ *Gan* mouse tumors compared to *Gan* mouse tumors (Fig. 6e).

Using *Apc*$^{Min/+}$ mice, we recently reported the role of VASH2 in the spontaneous formation of intestinal tumors. The *Vash2*-deficient *Apc*$^{Min/+}$ mice (*Vash2*$^{LacZ/LacZ}$ *Apc*$^{Min/+}$) showed a reduced number of polyps alongside the attenuation of tumor angiogenesis as compared to *Apc*$^{Min/+}$ mice.[10] We next carried out a DNA microarray analysis and identified 17 upregulated genes and 19 downregulated genes in intestinal polyps of *Vash2*$^{LacZ/LacZ}$ *Apc*$^{Min/+}$ mice compared with *Apc*$^{Min/+}$ mice (Tables S4 and S5). Comparative analysis of mRNA expression profiles obtained from *Gan* mouse gastric tumors and *Apc*$^{Min/+}$ intestinal polyps revealed that three genes (*Ereg*, *Il11* and *Tmem190*) were commonly downregulated in gastric tumors and intestinal polyps of *Vash2*-deficient mice (Fig. S1a). There was no overlap of upregulated genes (data not shown). Indeed, *Ereg* and *Il11* mRNA was significantly downregulated in polyps of *Vash2*$^{LacZ/LacZ}$ *Apc*$^{Min/+}$ mice compared to *Apc*$^{Min/+}$ mice (Fig. S1b), suggesting that VASH2 promotes expression of EREG and IL-11 in gastrointestinal tumorigenesis.

Suppression of fibroblast activation by knockdown of VASH2 in gastric cancer cells *in vitro*. We finally examined whether VASH2 expressed in human gastric cancer cells affects fibroblast expansion *in vitro*. The expression of *VASH2* mRNA in human gastric cancer cell line FU97 was significantly higher

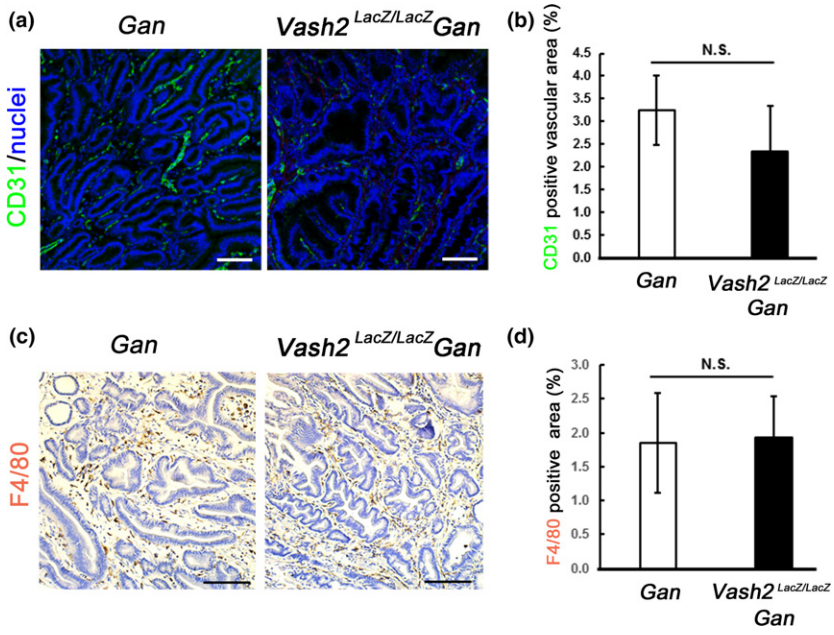

Fig. 4. Effect of *Vash2* depletion on tumor angiogenesis and macrophage infiltration. (a) Representative images of immunohistochemical staining for CD31 (green) of *Gan* mouse (left) and *Vash2*$^{LacZ/LacZ}$ *Gan* mouse (right) gastric tumors at 30 weeks of age. Nuclei were stained with TOPRO-3 (blue). Scale bars: 200 μm. (b) Quantification of the percentage of CD31-positive vascular vessel area to total tumor area ($n = 8$ fields analyzed from three independent animals). (c) Representative images of immunohistochemical staining for F4/80 of *Gan* mouse (left) and *Vash2*$^{LacZ/LacZ}$ *Gan* mouse (right) gastric tumors at 30 weeks of age. Counterstaining of nuclei was performed with hematoxylin. Scale bars: 200 μm. (d) Quantification of the percentage of F4/80 positive area to total tumor area ($n = 12$ fields analyzed from three independent animals). All quantitative data show mean ± SD. $^*P < 0.05$ versus *Gan* mouse tumors. N.S., not significant.

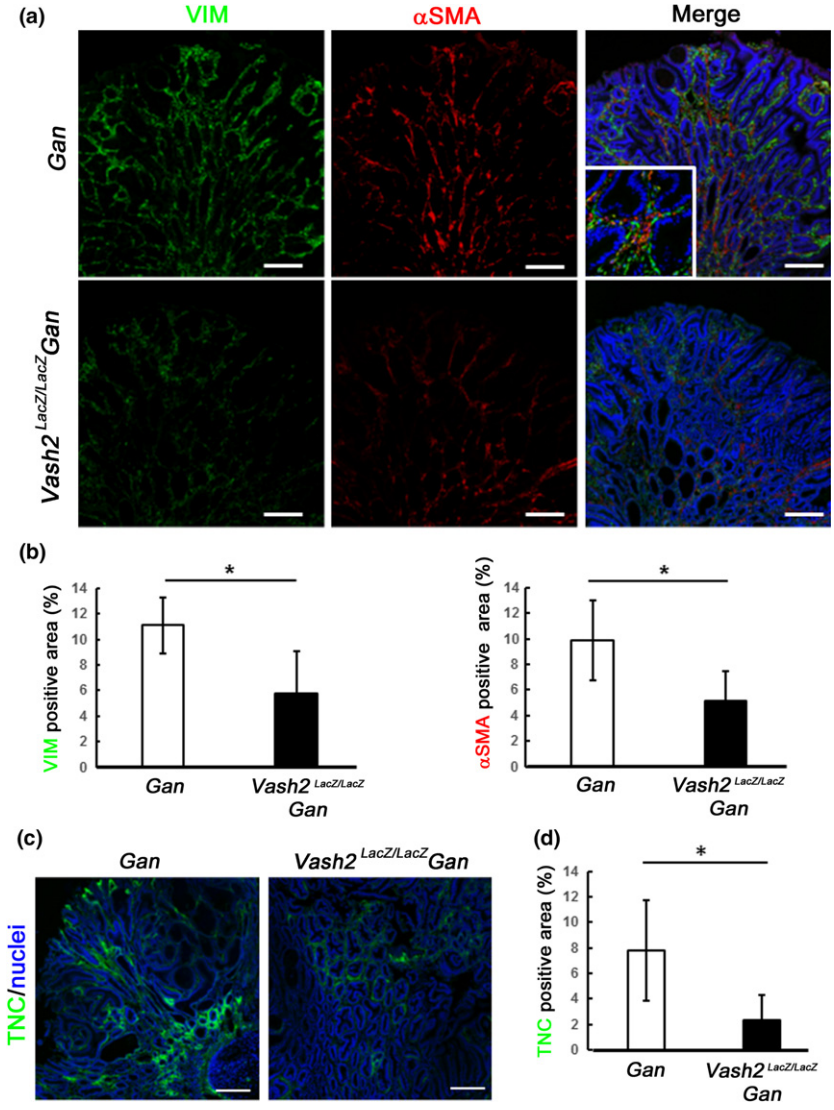

Fig. 5. Suppression of cancer-associated fibroblast expansion in gastric tumor stroma by *Vash2* knockout. (a) Representative images of a double-fluorescent immunostaining for αSMA and VIM of *Gan* and *Vash2*$^{LacZ/LacZ}$ *Gan* mouse gastric tumors at 30 weeks of age. Nuclei were stained with TOPRO-3 (blue). Scale bars: 200 μm. Inset, high magnification. (b) Quantification of the percentages of αSMA-positive and VIM-positive areas to total gastric tumor area ($n = 6$ fields analyzed from three independent animals). (c) Representative images of a fluorescent immunostaining for TNC of *Gan* and *Vash2*$^{LacZ/LacZ}$ *Gan* mouse gastric tumors at 30 weeks of age. Nuclei were stained with TOPRO-3 (blue). Scale bars: 200 μm. (d) Quantification of the percentage of TNC-positive area to total gastric tumor area ($n = 6$ fields analyzed from three independent animals). All quantitative data show mean ± SD. $^*P < 0.05$ versus *Gan* mouse tumors. N.S., not significant.

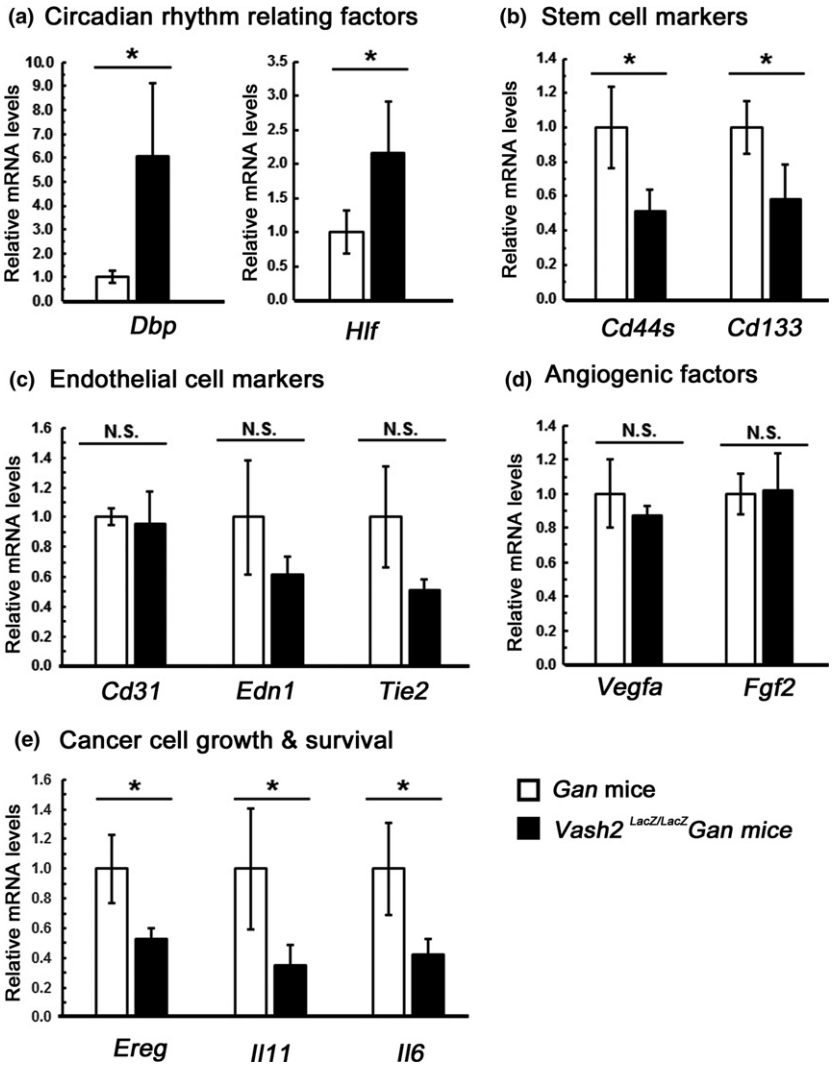

Fig. 6. *Vash2* depletion downregulates mRNA levels of *Ereg* and *Il11* in *Gan* mouse gastric tumors. The mRNA levels of indicated genes in gastric tumors of *Vash2*$^{LacZ/LacZ}$ *Gan* mouse at 30 weeks of age ($n = 4$) relative to those in gastric tumors of *Gan* mouse were determined by real-time RT-PCR analysis. The mRNA expression levels were normalized to *B2m* mRNA level. All quantitative data show mean ± SD. *$P < 0.05$ versus *Gan* mouse gastric tumors. N.S., not significant.

than that in human fibroblast SF-TY cells (Fig. 7a). We isolated VASH2 knockdown cell lines (shVASH2-1 and -2) using shRNA (Fig. 7b) and performed a loss-of-function experiment *in vitro*. CM of parent FU97 cells and mock control cells stimulated migration of and *ACTA2* (αSMA) expression in SF-TY cells (Fig. 7c,d). Importantly, CM of shVASH2 cells significantly attenuated the stimulatory effects. There was no significant effect on proliferation of SF-TY cells (Fig. 7c).

These results suggested that VASH2 produced by cancer cells influences CAF expansion and gastrointestinal tumor growth through upregulation of *EREG* and *IL-11*gene expression, in addition to its proangiogenic activity (Fig. 8).

Discussion

Previous studies have reported that VASH2 produced from cancer cells promotes tumor growth by stimulating tumor angiogenesis.[8,9] VASH2 is secreted from cancer cells and acts on neighboring vascular endothelial cells as a paracrine angiogenesis stimulator. Most studies on the role of VASH2 in tumor growth have used allograft and xenograft models of established cancer cell lines. In this work, we employed *Gan* mice as a spontaneous gastric tumor developmental model and confirmed that knockout of *Vash2* in *Gan* mice attenuates gastric tumor growth with a slight reduction in tumor angiogenesis. In addition to this proangiogenic activity, we found a novel role for VASH2 in the tumor stromal microenvironment, namely CAF. The increase in CAF is one of the characteristic features of gastric cancer in *Gan* mice.[19] *Vash2* depletion dramatically reduced the expansion of CAF in gastric tumor stroma along with downregulation of *Ereg*, *Il6* and *Il11* expression. We also confirmed that the expression of circadian genes (*Dbp*, *Hlf*, *Per3* and *Tef*) and of cancer stem cell markers (CD44 and CD133) is upregulated and downregulated, respectively, in *Vash2*$^{LacZ/LacZ}$ *Gan* mouse tumors. These changes might reflect suppression of tumor progression by knockout of *Vash2* because previous reports have shown downregulation of circadian genes in various tumors.[33–35]

Using the *Apc*$^{Min/+}$ mouse model, we recently demonstrated that *Vash2* depletion causes a reduced number of polyps alongside attenuation of tumor angiogenesis. Here, we also confirmed the reduced expression of *Ereg* and *Il11* in intestinal polyps of *Vash2*-deficient *Apc*$^{Min/+}$ mice as well as gastric tumors of *Vash2*-deficient *Gan* mice. EREG and IL-11 play a crucial role in gastrointestinal tumor growth, progression and chemoprevention through crosstalk between EGFR and gp130 signaling.[24,32,36–39] Enhanced expression of the *Ereg* gene has also been found in gastric cancer cells.[40] Oshima *et al.* report

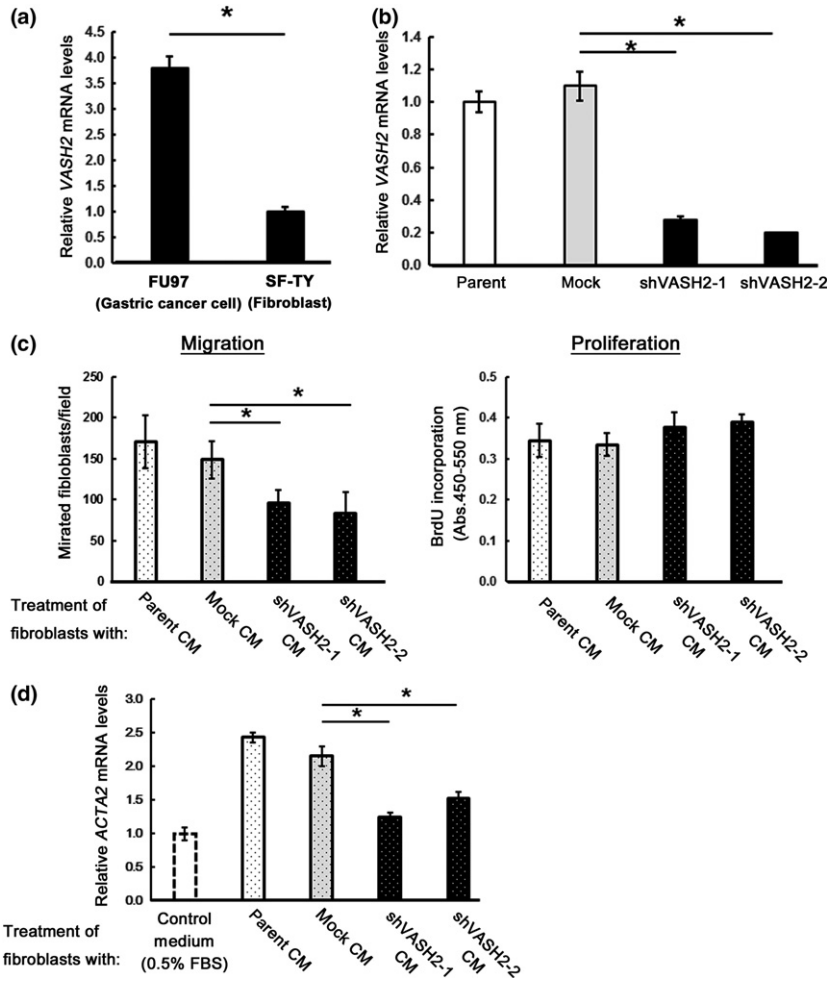

Fig. 7. Knockdown of VASH2 in gastric cancer cells suppresses fibroblast activation *in vitro*. (a) *VASH2* mRNA level in FU97 cells relative to that in SF-TY cells was determined by real-time RT-PCR analysis. The *VASH2* mRNA expression levels were normalized to β-*actin* mRNA level. $*P < 0.05$ versus SF-TY cell. (b) *VASH2* mRNA level in *VASH2* knockdown clones and control mock transfectant relative to that in parental FU97 cells was determined by real-time RT-PCR analysis. $*P < 0.05$ versus parental FU97 cell. (c) Effect of conditioned media (CM) of gastric cancer cells on fibroblast migration and proliferation. SF-TY cells were treated with CM of indicated gastric cancer cells. Migration and proliferation of SF-TY cells were analyzed by a modified Boyden chamber assay and BrdU incorporation assay, respectively. $*P < 0.05$ versus mock CM. (d) Effect of CM of gastric cancer cells on *ACTA2* mRNA expression in fibroblasts. The *ACTA2* mRNA levels in SF-TY cells treated with CM of indicated gastric cancer cells for 48 h were examined by real-time RT-PCR. $*P < 0.05$ versus mock CM. All quantitative data show mean ± SD. All experiments were performed at least twice.

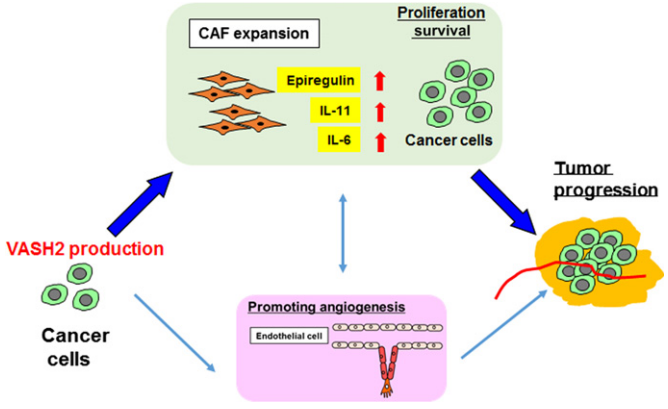

Fig. 8. Roles of VASH2 in gastric tumor growth. Schematic illustration of the roles of VASH2 in gastric tumor growth. VASH2 is produced from cancer cells and acts on neighboring EC as a proangiogenic factor in a paracrine manner. In contrast, VASH2 influences cancer cell proliferation and stromal activation, such as CAF expansion, by upregulating the expression of *EREG*, *IL-11* and *IL-6*.

PGE_2 pathway-dependent Ereg expression by gastric epithelial cells and macrophages in *Gan* mouse gastric tumors.[24] Of importance, other recent reports have suggested that CAF as well as cancer cells are a major supplier of Ereg and IL-11 in tumor stroma.[37–39,41,42] In this study, we showed that *Vash2* disruption influences CAF expansion but not a population of macrophages infiltrating into the gastric tumor stroma. Therefore, it is possible that VASH2 stimulates the expression of EREG and IL-11 in CAF and cancer cells.

Cancer associated fibroblasts in *Gan* mice produce VEGFA and promote tumor angiogenesis;[21] however, our data showed that *Vash2* depletion did not affect *Vegfa* mRNA level despite reduced CAF expansion. We performed double immunostaining for αSMA and VIM and observed three types of CAF subpopulations (αSMA-positive, VIM-positive and double-positive cells), suggesting that CAF are a heterogeneous population in the tumor microenvironment.[43,44] Öhlund *et al.* recently identified distinct populations of inflammatory and myofibroblastic CAF in pancreatic cancer. The inflammatory CAF had low αSMA expression and concomitantly produced inflammatory factors, such as IL-6, IL-11 and leukemia inhibitory factor.[42] Therefore, it is possible that VASH2 may specifically affect certain subtypes of CAF that express higher levels of IL-11and/or EREG than other subtypes.

Transforming growth factor-β (TGF-β) signal is one of the most important pathways for CAF activation as well as tumor metastasis. VASH2 has been recently reported to be involved in epithelial–mesenchymal transition and the chemoprevention ability of cancer cells.[18,45–47] We earlier found that VASH2 might accelerate TGF-β-induced epithelial–mesenchymal transition and invasiveness of ovarian cancer cells by modulating TGF-β type I receptor expression, suggesting functional

links between TGF-β signal and VASH2 action in tumor progression.[45]

In summary, we propose that VASH2 plays an important role in tumor progression via stromal activation, such as CAF expansion, by upregulating the expression of EREG and IL-11, in addition to its proangiogenic activity (Fig. 8). Further studies are currently under way to clarify the molecular mechanism by which VASH2 causes stromal activation. It is also possible that targeting of VASH2 may be applied as a novel molecular target therapy for gastric cancers, which is also under investigation.

Acknowledgments

We wish to thank Y. Fujinoya for excellent technical assistance. This study was supported by JSPS KAKENHI Grant Numbers 24501309 and 15K06821.

Disclosure Statement

The authors have no conflict of interest to declare.

References

1 Berger H, Marques MS, Zietlow R, Meyer TF, Machado JC, Figueiredo C. Gastric cancer pathogenesis. *Helicobacter* 2016; **21**(Suppl 1): 34–8.
2 Shitara K, Ohtsu A. Advances in systemic therapy for metastatic or advanced gastric cancer. *J Natl Compr Canc Netw* 2016; **14**: 1313–20.
3 Watanabe K, Hasegawa Y, Yamashita H *et al.* Vasohibin as an endothelium-derived negative feedback regulator of angiogenesis. *J Clin Invest* 2004; **114**: 898–907.
4 Kimura H, Miyashita H, Suzuki Y *et al.* Distinctive localization and opposed roles of vasohibin-1 and vasohibin-2 in the regulation of angiogenesis. *Blood* 2009; **113**: 4810–8.
5 Shibuya T, Watanabe K, Yamashita H *et al.* Isolation and characterization of vasohibin-2 as a homologue of VEGF-inducible endothelium-derived angiogenesis inhibitor vasohibin. *Arterioscler Thromb Vasc Biol* 2006; **26**: 1051–7.
6 Suzuki Y, Kobayashi M, Miyashita H, Ohta H, Sonoda H, Sato Y. Isolation of a small vasohibin-binding protein (SVBP) and its role in vasohibin secretion. *J Cell Sci* 2010; **123**: 3094–101.
7 Kadonosono T, Yimchuen W, Tsubaki T *et al.* Domain architecture of vasohibins required for their chaperone-dependent unconventional extracellular release. *Protein Sci* 2017; **26**: 452–63.
8 Takahashi Y, Koyanagi T, Suzuki Y *et al.* Vasohibin-2 expressed in human serous ovarian adenocarcinoma accelerates tumor growth by promoting angiogenesis. *Mol Cancer Res* 2012; **10**: 1135–46.
9 Xue X, Gao W, Sun B *et al.* Vasohibin 2 is transcriptionally activated and promotes angiogenesis in hepatocellular carcinoma. *Oncogene* 2013; **32**: 1724–34.
10 Kitahara S, Suzuki Y, Morishima M *et al.* Vasohibin-2 modulates tumor onset in the gastrointestinal tract by normalizing tumor angiogenesis. *Mol Cancer* 2014; **13**: 99.
11 Koyanagi T, Suzuki Y, Saga Y *et al. In vivo* delivery of siRNA targeting vasohibin-2 decreases tumor angiogenesis and suppresses tumor growth in ovarian cancer. *Cancer Sci* 2013; **104**: 1705–10.
12 Koyanagi T, Suzuki Y, Komori K *et al.* Targeting human vasohibin-2 by a neutralizing monoclonal antibody for anti-cancer treatment. *Cancer Sci* 2016; **108**: 512–9.
13 Shen Z, Kauttu T, Seppänen H *et al.* Vasohibin-1 and vasohibin-2 expression in gastric cancer cells and TAMs. *Med Oncol* 2012; **29**: 2718–26.
14 Oshima H, Matsunaga A, Fujimura T, Tsukamoto T, Taketo MM, Oshima M. Carcinogenesis in mouse stomach by simultaneous activation of the Wnt signaling and prostaglandin E2 pathway. *Gastroenterology* 2006; **131**: 1086–95.
15 Ishimoto T, Oshima H, Oshima M *et al.* CD44+ slow-cycling tumor cell expansion is triggered by cooperative actions of Wnt and prostaglandin E2 in gastric tumorigenesis. *Cancer Sci* 2010; **101**: 673–8.
16 Kim JC, Kim KT, Park JT, Kim HJ, Sato Y, Kim HS. Expression of vasohibin-2 in pancreatic ductal adenocarcinoma promotes tumor progression and is associated with a poor clinical outcome. *Hepatogastroenterology* 2015; **62**: 251–6.
17 Koyanagi T, Saga Y, Takahashi Y, Suzuki Y, Suzuki M, Sato Y. Downregulation of vasohibin-2, a novel angiogenesis regulator, suppresses tumor growth by inhibiting angiogenesis in endometrial cancer cells. *Oncol Lett* 2013; **5**: 1058–62.
18 Li Z, Tu M, Han B *et al.* Vasohibin 2 decreases the cisplatin sensitivity of hepatocarcinoma cell line by downregulating p53. *PLoS ONE* 2014; **9**: e90358.
19 Xue X, Zhang Y, Zhi Q *et al.* MiR200-upregulated Vasohibin 2 promotes the malignant transformation of tumors by inducing epithelial–mesenchymal transition in hepatocellular carcinoma. *Cell Commun Signal* 2014; **12**: 62.
20 Ge Q, Zhou J, Tu M *et al.* Nuclear vasohibin-2 promotes cell proliferation by inducing G0/G1 to S phase progression. *Oncol Rep* 2015; **34**: 1327–36.
21 Guo X, Oshima H, Kitmura T, Taketo MM, Oshima M. Stromal fibroblasts activated by tumor cells promote angiogenesis in mouse gastric cancer. *J Biol Chem* 2008; **283**: 19864–71.
22 Kong D, Piao YS, Yamashita S *et al.* Inflammation-induced repression of tumor suppressor miR-7 in gastric tumor cells. *Oncogene* 2012; **31**: 3949–60.
23 Maeda Y, Echizen K, Oshima H *et al.* Myeloid differentiation factor 88 signaling in bone marrow-derived cells promotes gastric tumorigenesis by generation of inflammatory microenvironment. *Cancer Prev Res (Phila)* 2016; **9**: 253–63.
24 Oshima H, Popivanova BK, Oguma K, Kong D, Ishikawa TO, Oshima M. Activation of epidermal growth factor receptor signaling by the prostaglandin E(2) receptor EP4 pathway during gastric tumorigenesis. *Cancer Sci* 2011; **102**: 713–9.
25 Oshima H, Hioki K, Popivanova BK *et al.* Prostaglandin E_2 signaling and bacterial infection recruit tumor-promoting macrophages to mouse gastric tumors. *Gastroenterology* 2011; **140**: 596–607.e7.
26 Oshima H, Oshima M. The role of PGE2-associated inflammatory responses in gastric cancer development. *Semin Immunopathol* 2013; **35**: 139–50.
27 Oshima H, Ishikawa T, Yoshida GJ *et al.* TNF-α/TNFR1 signaling promotes gastric tumorigenesis through induction of Noxo1 and Gna14 in tumor cells. *Oncogene* 2014; **33**: 3820–9.
28 Ishimoto T, Nagano O, Yae T *et al.* CD44 variant regulates redox status in cancer cells by stabilizing the xCT subunit of system xc(-) and thereby promotes tumor growth. *Cancer Cell* 2011; **19**: 387–400.
29 Bollrath J, Phesse TJ, von Burstin VA *et al.* gp130-mediated Stat3 activation in enterocytes regulates cell survival and cell-cycle progression during colitis-associated tumorigenesis. *Cancer Cell* 2009; **15**: 91–102.
30 Grivennikov SI. IL-11: a prominent pro-tumorigenic member of the IL-6 family. *Cancer Cell* 2013; **24**: 145–7.
31 Nagasaki T, Hara M, Nakanishi H, Takahashi H, Sato M, Takeyama H. Interleukin-6 released by colon cancer-associated fibroblasts is critical for tumour angiogenesis: anti-interleukin-6 receptor antibody suppressed angiogenesis and inhibited tumour–stroma interaction. *Br J Cancer* 2014; **110**: 469–78.
32 Putoczki TL, Thiem S, Loving A *et al.* Interleukin-11 is the dominant IL-6 family cytokine during gastrointestinal tumorigenesis and can be targeted therapeutically. *Cancer Cell* 2013; **24**: 257–71.
33 Cadenas C, van de Sandt L, Edlund K *et al.* Loss of circadian clock gene expression is associated with tumor progression in breast cancer. *Cell Cycle* 2014; **13**: 3282–91.
34 Lin YM, Chang JH, Yeh KT *et al.* Disturbance of circadian gene expression in hepatocellular carcinoma. *Mol Carcinog* 2008; **47**: 925–33.
35 Soták M, Polidarová L, Ergang P, Sumová A, Pácha J. An association between clock genes and clock-controlled cell cycle genes in murine colorectal tumors. *Int J Cancer* 2013; **132**: 1032–41.
36 Ernst M, Najdovska M, Grail D *et al.* STAT3 and STAT1 mediate IL-11-dependent and inflammation-associated gastric tumorigenesis in gp130 receptor mutant mice. *J Clin Invest* 2008; **118**: 1727–38.
37 Tao L, Huang G, Wang R *et al.* Cancer-associated fibroblasts treated with cisplatin facilitates chemoresistance of lung adenocarcinoma through IL-11/IL-11R/STAT3 signaling pathway. *Sci Rep* 2016; **6**: 38408.
38 Neufert C, Becker C, Türeci Ö *et al.* Tumor fibroblast-derived epiregulin promotes growth of colitis-associated neoplasms through ERK. *J Clin Invest* 2013; **123**: 1428–43.
39 Calon A, Espinet E, Palomo-Ponce S *et al.* Dependency of colorectal cancer on a TGF-β-driven program in stromal cells for metastasis initiation. *Cancer Cell* 2012; **22**: 571–84.
40 Riese DJ, Cullum RL. Epiregulin: roles in normal physiology and cancer. *Semin Cell Dev Biol* 2014; **28**: 49–56.
41 Yoshikawa M, Kojima H, Yaguchi Y, Okada N, Saito H, Moriyama H. Cholesteatoma fibroblasts promote epithelial cell proliferation through overexpression of epiregulin. *PLoS ONE* 2013; **8**: e66725.

42 Öhlund D, Handly-Santana A, Biffi G *et al.* Distinct populations of inflammatory fibroblasts and myofibroblasts in pancreatic cancer. *J Exp Med* 2017; **214**: 579–96.
43 Kalluri R. The biology and function of fibroblasts in cancer. *Nat Rev Cancer* 2016; **16**: 582–98.
44 Li H, Courtois ET, Sengupta D *et al.* Reference component analysis of single-cell transcriptomes elucidates cellular heterogeneity in human colorectal tumors. *Nat Genet* 2017; **49**: 708–18.
45 Norita R, Suzuki Y, Furutani Y *et al.* Vasohibin-2 is required for epithelial–mesenchymal transition of ovarian cancer cells by modulating TGF-β signaling. *Cancer Sci* 2017; **108**: 419–26.
46 Tu M, Li Z, Liu X *et al.* Vasohibin 2 promotes epithelial–mesenchymal transition in human breast cancer via activation of transforming growth factor β 1 and hypoxia dependent repression of GATA-binding factor 3. *Cancer Lett* 2017; **388**: 187–97.
47 Tu M, Li H, Lv N *et al.* Vasohibin 2 reduces chemosensitivity to gemcitabine in pancreatic cancer cells via Jun proto-oncogene dependent transactivation of ribonucleotide reductase regulatory subunit M2. *Mol Cancer* 2017; **16**: 66.

Supporting Information

Additional Supporting Information may be found online in the supporting information tab for this article:

Fig. S1. *Vash2* disruption commonly downregulates *Ereg* and *Il11* genes in mouse gastric tumors and intestinal polyps.

Table S1. Primers used for RT-PCR and real-time RT-PCR analysis.

Table S2. Genes upregulated in gastric tumors of *Vash2*-deficient *Gan* mice.

Table S3. Genes downregulated in gastric tumors of *Vash2*-deficient *Gan* mice.

Table S4. Genes upregulated in intestinal polyps of *Vash2*-deficient $Apc^{Min/+}$ mice.

Table S5. Genes downregulated in intestinal polyps of *Vash2*-deficient $Apc^{Min/+}$ mice.